AMERICAN SOCIETY FOR MICROBIOLOGY | Journal of Virology®

VIRUS-CELL INTERACTIONS

A Tyrosine-Based Trafficking Motif of the Tegument Protein pUL71 Is Crucial for Human Cytomegalovirus Secondary Envelopment

Andrea N. Dietz,[a] Clarissa Villinger,[a,b] Stefan Becker,[a] Manfred Frick,[c] Jens von Einem[a]

[a]Institute of Virology, Ulm University Medical Center, Ulm, Germany
[b]Central Facility for Electron Microscopy, Ulm University, Ulm, Germany
[c]Institute of General Physiology, Ulm University, Ulm, Germany

ABSTRACT The human cytomegalovirus (HCMV) tegument protein pUL71 is required for efficient secondary envelopment and accumulates at the Golgi compartment-derived viral assembly complex (vAC) during infection. Analysis of various C-terminally truncated pUL71 proteins fused to enhanced green fluorescent protein (eGFP) identified amino acids 23 to 34 as important determinants for its Golgi complex localization. Sequence analysis and mutational verification revealed the presence of an N-terminal tyrosine-based trafficking motif (YXXΦ) in pUL71. This led us to hypothesize a requirement of the YXXΦ motif for the function of pUL71 in infection. Mutation of both the tyrosine residue and the entire YXXΦ motif resulted in an altered distribution of mutant pUL71 at the plasma membrane and in the cytoplasm during infection. Both YXXΦ mutant viruses exhibited similarly decreased focal growth and reduced virus yields in supernatants. Ultrastructurally, mutant-virus-infected cells exhibited impaired secondary envelopment manifested by accumulations of capsids undergoing an envelopment process. Additionally, clusters of capsid accumulations surrounding the vAC were observed, similar to the ultrastructural phenotype of a UL71-deficient mutant. The importance of endocytosis and thus the YXXΦ motif for targeting pUL71 to the Golgi complex was further demonstrated when clathrin-mediated endocytosis was inhibited either by coexpression of the C-terminal part of cellular AP180 (AP180-C) or by treatment with methyl-β-cyclodextrin. Both conditions resulted in a plasma membrane accumulation of pUL71. Altogether, these data reveal the presence of a functional N-terminal endocytosis motif that is an important determinant for intracellular localization of pUL71 and that is furthermore required for the function of pUL71 during secondary envelopment of HCMV capsids at the vAC.

IMPORTANCE Human cytomegalovirus (HCMV) is the leading cause of birth defects among congenital virus infections and can lead to life-threatening infections in immunocompromised hosts. Current antiviral treatments target viral genome replication and are increasingly overcome by viral mutations. Therefore, identifying new targets for antiviral therapy is important for future development of novel treatment options. A detailed molecular understanding of the complex virus morphogenesis will identify potential viral as well as cellular targets for antiviral intervention. Secondary envelopment is an important viral process through which infectious virus particles are generated and which involves the action of several viral proteins, such as tegument protein pUL71. Targeting of pUL71 to the site of secondary envelopment appears to be crucial for its function during this process and is regulated by utilizing host trafficking mechanisms that are commonly exploited by viral glycoproteins. Thus, intracellular trafficking, if targeted, might present a novel target for antiviral therapy.

Received 2 June 2017 **Accepted** 3 October 2017

Accepted manuscript posted online 18 October 2017

Citation Dietz AN, Villinger C, Becker S, Frick M, von Einem J. 2018. A tyrosine-based trafficking motif of the tegument protein pUL71 is crucial for human cytomegalovirus secondary envelopment. J Virol 92:e00907-17. https://doi.org/10.1128/JVI.00907-17.

Editor Richard M. Longnecker, Northwestern University

Address correspondence to Jens von Einem, jens.von-einem@uniklinik-ulm.de.

KEYWORDS HCMV, cytomegalovirus, endocytosis, intracellular trafficking, morphogenesis, secondary envelopment, tegument, trafficking signal

Human cytomegalovirus (HCMV) is a member of the *Betaherpesvirinae* subfamily and one of the few viruses within the *Herpesviridae* family known to be restricted to humans. HCMV is greatly adapted to its human host and can cause life-threatening diseases in neonates and immunocompromised individuals, such as transplant recipients and AIDS patients (reviewed in reference 1).

HCMV virions have the typical herpesvirus morphology consisting of the genome containing the icosahedral capsid, the tegument, and the envelope. The envelope is a cell-derived lipid bilayer in which several virus-encoded glycoproteins and glycoprotein complexes are incorporated. The tegument is a proteinaceous layer connecting the capsid and the envelope (2). The tegument consists of more than 38 virus-encoded tegument proteins, representing around 50% of the total protein amount of the virion (3, 4), associated cellular proteins, and RNA (4, 5). The general mechanism by which HCMV virions are generated is conserved among herpesviruses (reviewed in references 6 and 7). The last step of virion morphogenesis, resulting in the generation of infectious virus particles, is referred to as secondary envelopment. Secondary envelopment describes the process through which cytoplasmic virus capsids acquire their envelope by budding into cytoplasmic vesicles. In the case of HCMV, secondary envelopment occurs at the viral assembly complex (vAC) (8). The vAC is formed during infection at the indentation of a kidney-shaped nucleus by rearrangement of the Golgi complex and endocytic membranes (8–10). The large numbers of viral proteins which are incorporated into virions require a well-coordinated trafficking of these proteins to the vAC as well as a vast interplay of protein-protein interactions (11). It was previously suggested that HCMV utilizes different trafficking pathways to target virus-encoded proteins to the vAC (12). However, we have not fully understood which viral protein is using which trafficking pathway. Intracellular trafficking of glycoproteins has been shown to be regulated by the presence of trafficking signals in their cytoplasmic tails. An important part of glycoprotein trafficking is endocytosis from the plasma membrane mediated by endocytic trafficking signals (13–23). One family of such a motif is the tyrosine-based trafficking motif YXXΦ (X stands for any amino acid; Φ stands for an amino acid with a bulky hydrophobic side chain) (24–27). YXXΦ motifs were shown to be involved in receptor internalization from the plasma membrane (28) and protein targeting to lysosomes (29), endosomal compartments (30–32), the basolateral surface of polarized cells (33), and the *trans*-Golgi network (TGN) (34–36). At the plasma membrane YXXΦ motifs are recognized by the μ2 subunit of the adaptor protein complex 2 (AP-2), which recruits proteins to clathrin-coated pits and thus to clathrin-coated vesicles (37). In addition to glycoproteins, several herpesvirus tegument proteins are known to be associated with cellular membranes (8, 38, 39). One important protein for HCMV virion morphogenesis is the tegument protein pUL71, which accumulates at the vAC in infected cells. It was shown that pUL71 is required for efficient secondary envelopment of capsids at the vAC as in its absence the majority of capsids in the vAC were found in various stages of incomplete envelopment (40, 41). Consistent with an impaired envelopment of cytoplasmic capsids, virus release and virus spread in tissue culture were markedly reduced (41, 42). The function of pUL71 in secondary envelopment appears to be conserved among herpesviruses since absence of the homologous protein pUL51 in pseudorabies virus (PRV) and herpes simplex virus 1 (HSV-1) results in defects in secondary envelopment (43, 44). It was also shown that pUL51 partially colocalizes with Golgi complex markers during infection and that its Golgi complex localization requires palmitoylation of an N-terminal cysteine residue (38). It has been recognized previously that pUL71 homologues contain a conserved YXXΦ motif near the N terminus, which is critical for the HSV-1 pUL51 cell-to-cell spread function in HEp-2 cells (45). Considering the intracellular trafficking potential of membrane-associated proteins (46), the vAC localization of HCMV pUL71 (40, 42), and its obvious

function at membranes for the membrane fusion around viral particles, we addressed whether intracellular trafficking of pUL71 to the vAC is regulated by trafficking signals. We utilized a genetic approach to identify specific domains of HCMV pUL71 regulating its Golgi complex localization. We thereby identified an N-terminal YXXΦ motif in pUL71, which meditates clathrin-mediated endocytosis of pUL71. We furthermore investigated the role of this motif for the localization of pUL71 in infection and its function for viral growth and virion morphogenesis. Our results indicate that endocytosis is an important pathway for the targeting of pUL71 to the vAC and seems to be required for pUL71 function during secondary envelopment and virus replication.

RESULTS

Changes in intracellular localization of C-terminally truncated pUL71. In order to identify functional domains with importance for intracellular trafficking of HCMV tegument protein pUL71, C-terminally truncated fragments of pUL71 fused to enhanced green fluorescence protein (eGFP; yielding pUL71eGFP) were generated (Fig. 1A), and their intracellular localizations were examined in transiently expressing HeLa cells. These studies revealed that the N-terminal region comprising amino acids 22 to 34 is crucial for Golgi complex localization of pUL71, as indicated by signals that overlap those of the TGN marker protein TGN46 (Fig. 1B). Sequence analysis revealed the presence of a tyrosine-based trafficking signal (YXXΦ motif) at residues 23 to 26, which is present in the pUL71eGFP fragment consisting of residues 1 to 34 (pUL71eGFP_1–34) but absent in the fragment consisting of residues 1 to 22 (pUL71eGFP_1–22). A sequence alignment showed conservation of the N-terminal YXXΦ motif among UL71 homologues of other herpesviruses across all three herpesvirus subfamilies, consistent with previous results (45) (Fig. 2). To verify the importance of this motif for localization in the context of full-length pUL71, two different mutants were generated by either mutating the entire motif to alanines (pUL71eGFP_23–26A) or by exchanging the tyrosine for an alanine (pUL71eGFP_Y23A). Transient expression of pUL71eGFP_Y23A as well as of pUL71eGFP_23–26A in HeLa cells resulted in a dominant plasma membrane localization of mutated pUL71, whereas wild-type pUL71 predominantly localized at the Golgi compartment (Fig. 1B and C). A mutation of the tyrosine residue of the YXXΦ motif is seldom tolerated and usually disables functionality of this motif (23). Only a substitution with the very similar phenylalanine is tolerated in some cases (47, 48). In order to rescue the trafficking defect of mutation Y23A, we generated a mutant in which the tyrosine was replaced with phenylalanine (pUL71eGFP_Y23F). In transient expression, pUL71eGFP_Y23F exhibited localization at the Golgi complex similar to that of wild-type pUL71, indicating rescue of the trafficking motif (Fig. 1B and C). From this, we inferred the presence of a tyrosine-based trafficking signal in HCMV pUL71 with an important function in targeting this protein to the TGN.

Generation and growth analysis of YXXΦ mutant viruses. It has been shown previously that pUL71 is localized at the viral assembly complex (vAC) during infection where it has an important function in secondary envelopment (40, 42). Therefore, we assumed that trafficking of pUL71 to the site of secondary envelopment is critical for its function and thus virus growth. To address this, two different YXXΦ mutant viruses were constructed by either mutating the entire motif to alanines in TB-UL71mut23–26A or by exchanging only the tyrosine for an alanine in TB-UL71mutY23A (Fig. 3A). Additionally, a revertant virus, TB-UL71revY23A, was generated by reversing the point mutation Y23A back to a tyrosine and simultaneously introducing a silent mutation which makes it possible to distinguish between the revertant virus and the parental virus, referred to here as the wild type. Impairment in virus growth was already noticed for the two YXXΦ mutant viruses during virus reconstitution compared to growth of simultaneously reconstituted wild-type and revertant viruses. A subsequent detailed growth analyses revealed a significant defect in focal growth in a focus expansion assay at 7 days postinfection (dpi) (Fig. 3B and C). The YXXΦ mutant viruses TB-UL71mut23–26A and TB-UL71mutY23A formed foci with a mean of 15 and 16 immediate early 1 and 2 (IE1/2) protein-positive cells per focus compared to 33 and 30 IE-positive cells per

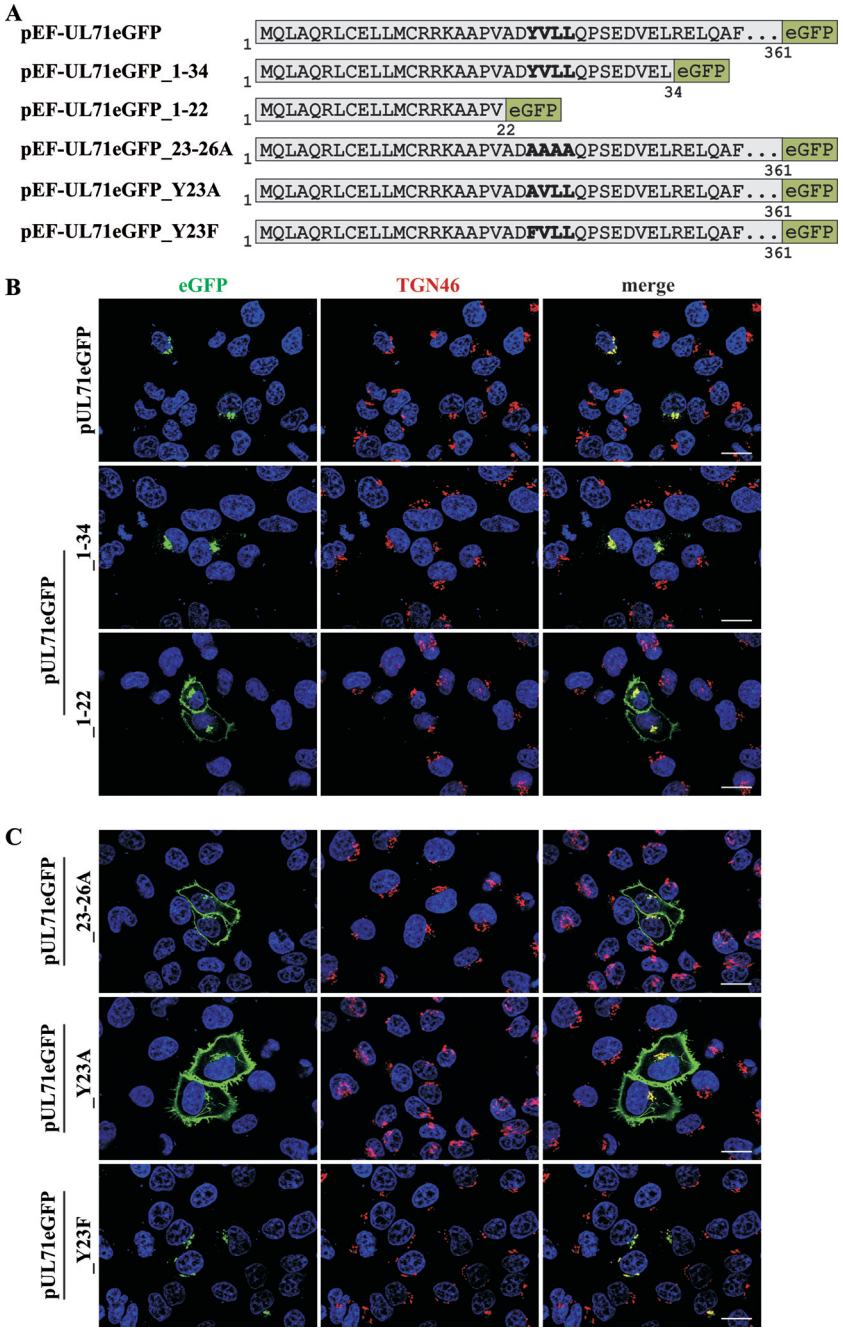

FIG 1 Generation and intracellular localization of pUL71 truncations. (A) Schematic of pUL71 fragments fused to eGFP expressed from the indicated expression plasmids. The sequence in bold indicates the YXXΦ motif in pUL71 fragments as well as the mutated motif in pUL71eGFP_23–26A, pUL71eGFP_Y23A, and pUL71eGFP_Y23F. HeLa cells transiently expressing full-length pUL71eGFP and the two pUL71 fragments, pUL71eGFP_1–34 and pUL71eGFP_1–22 (B) as well as YXXΦ motif mutants, pUL71eGFP_23–26A, pUL71eGFP_Y23A, and pUL71eGFP_Y23F (C), were stained for TGN46 and cell nuclei with DAPI at 20 h posttransfection. Scale bar, 20 μm.

focus for wild-type and revertant viruses, respectively (Fig. 3B). The defect in focal growth of TB-UL71mut23–26A and TB-UL71mutY23A was similar to that of a pUL71-deficient virus (TB-UL71stop). To exclude potential functions of the YXXΦ motif other than endocytosis, mutant virus TB-UL71mutY23F was generated by exchanging the tyrosine for a phenylalanine (Fig. 3A). Viral growth in a focus expansion assay of TB-UL71mutY23F was similar to growth of the wild-type virus and revertant viruses

FIG 2 Amino acid sequence alignment of HCMV pUL71 homologues. The N-terminal amino acid sequence of residues 1 to 34 of HCMV pUL71 was aligned to pUL71 homologues of other herpesviruses using the online tool MUSCLE (69). Homologous proteins (square brackets) from human herpesviruses of all three subfamilies, *Alpha-*, *Beta-*, and *Gammaherpesvirinae*, show a highly conserved N-terminal YXXΦ trafficking signal (bold), where X stands for any amino acid and Φ stands for an amino acid with a bulky hydrophobic side chain. HHV, human herpesvirus; EBV, Epstein-Barr virus; VSV, vesicular stomatitis virus.

(Fig. 3B), indicating rescue of the YXXΦ motif in this mutant. Virus growth was further assessed in a multistep growth kinetics analysis by coculture of infected with noninfected fibroblasts (Fig. 3D). Virus yields in the supernatants of TB-UL71mut23–26A and TB-UL71mutY23A viruses were decreased at least 100-fold compared to those of wild-type and revertant viruses. Similar growth of TB-UL71mut23–26A and TB-UL71mutY23A further suggested an important function of the N-terminal YXXΦ motif for viral growth. In addition, similar growth of wild-type virus and the TB-UL71revY23A virus indicated that the mutation of the YXXΦ motif was successfully repaired.

Altered localization patterns of tegument proteins in mutant viruses. Next, we addressed whether mutation of the YXXΦ motif affects intracellular distribution of pUL71 in TB-UL71mut23–26A- and TB-UL71mutY23A-infected cells. As shown in Fig. 4, mutation of the tyrosine as well as of the entire YXXΦ motif resulted in altered distribution of mutant pUL71 in infected cells. Whereas pUL71 in wild-type, revertant, and TB-UL71mutY23F virus-infected cells primarily accumulated perinuclearly at the site of the vAC, signals of pUL71 in TB-UL71mut23–26A- and TB-UL71mutY23A-infected cells were found more in the cytoplasm and noticeably at the plasma membrane. This verified an important role of the YXXΦ motif for intracellular localization of pUL71 in infection. We have recently shown that the absence of pUL71 in a UL71-deficient virus infection is often accompanied by accumulations of other viral tegument proteins, such as pp28, at vesicular structures adjacent to the vAC (40). Assuming that these accumulations are the result of defects in the function of pUL71, we investigated if the altered pUL71 localization in YXXΦ mutant infections causes similar effects on pp28. As shown in Fig. 4, many, but not all, infected cells showed pp28 signals at vesicular structures in the area of the vAC that were also stained positive with 4′,6′-diamidino-2-phenylindole (DAPI) and were usually not found in wild-type, revertant, and TB-UL71mutY23F virus-infected cells.

Secondary envelopment is impaired in YXXΦ mutant viruses. The underlying cause of the growth and release impairment of a UL71-deficient mutant is based on a defect in secondary envelopment of virus particles (40, 41). Based on this, we hypothesized a similar cause for the impaired growth of YXXΦ mutant viruses. In order to visualize possible defects on secondary envelopment, we performed electron microscopy of virus-infected cells at 120 h postinfection (hpi). In an area corresponding to the vAC, increased numbers of larger tubular membrane structures and accumulations of virus particles were observed in TB-UL71mut23–26A- and TB-UL71mutY23A-infected cells (Fig. 5). In addition, multiple budding events of viral particles were observed at these tubular structures, whereas in wild-type-infected cells, single capsids were observed typically in budding processes at small vesicles (Fig. 5B). Budding events in wild-type infection, however, are less frequently observed because the majority of capsids have already acquired an envelope. Quantification of secondary envelopment stages showed clear differences in the numbers of capsids undergoing envelopment among YXXΦ mutant-infected fibroblasts and wild-type virus (Table 1). Stages of secondary envelopment were divided into three categories and quantified from a minimum of 10 infected cells for each virus. Category 1 comprised fully enveloped particles, category 2 consisted of capsids associated with membranes but not fully

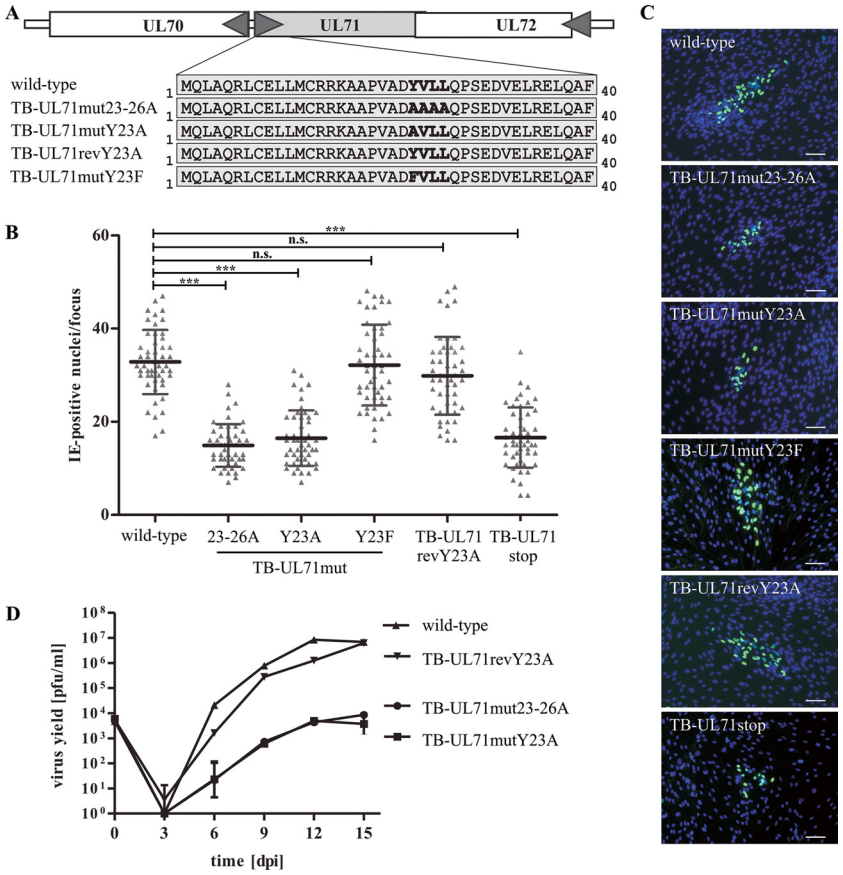

FIG 3 Generation and growth analysis of YXXΦ mutant viruses. (A) Shown are the genomic organization down- and upstream of the UL71 gene and the amino acid sequence of the pUL71 N terminus of the wild-type virus, YXXΦ mutant viruses, and the revertant virus, respectively. The YXXΦ motif as well as the introduced mutations within this motif is shown in bold. (B) Focus expansion assay of the indicated viruses in HFF under methylcellulose overlay. HCMV-infected cells were detected by indirect immunofluorescence staining for IE1/2 antigen at 7 dpi. Each data point represents the number of IE1/2-positive cell nuclei per focus. Shown is the mean value of 50 foci for each virus for one of three experiments or, in the case of the TB-UL71mutY23F and TB-UL71stop viruses, for one of two experiments. Significance was determined by applying a two-tailed Student *t* test (***, $P < 0{,}0001$; n.s., not significant). (C) Images of representative foci of the indicated viruses at 7 dpi under methylcellulose overlay. IE1/2-positive cells were detected by an anti-IE1/2 antibody and visualized by an Alex Fluor 488-conjugated secondary antibody. Cell nuclei were stained with DAPI. Scale bar, 100 μm. (D) Multistep growth kinetics analyses of the indicated viruses were performed by infecting HFF at an MOI of 0.02 by coseeding of infected with uninfected cells. Virus yields in the supernatants of infected cells were determined at the indicated times by titration on HFF. Growth curves show the mean virus yields and standard deviations of three independent virus supernatants. Virus yields at time zero represent the starting infection rates determined at 24 h postcoseeding.

enclosed with a membrane, and category 3 was comprised of free capsids not attached to any membrane. Consistent with previous data of a UL71-deficient virus, an average of around 10-fold-higher numbers of virus particles was counted per vAC area in both YXXΦ mutant infections than in wild-type virus infections. Of these particles, ~83% and ~76% were capsids undergoing secondary envelopment (category 2) in TB-UL71mut23–26A- and TB-UL71mutY23A-infected cells, respectively, in contrast to ~35% in wild-type virus infection. These data show an impaired secondary envelopment in TB-UL71mut23–26A and TB-UL71mutY23A infection with a lower proportion of fully enveloped particles resulting in increased numbers of capsids at the vAC. This underlines the importance of intracellular localization of pUL71 at the vAC for HCMV virion morphogenesis.

Inhibition of endocytosis results in accumulation of pUL71 at the plasma membrane. YXXΦ motifs are known to be involved in endocytosis of proteins from the

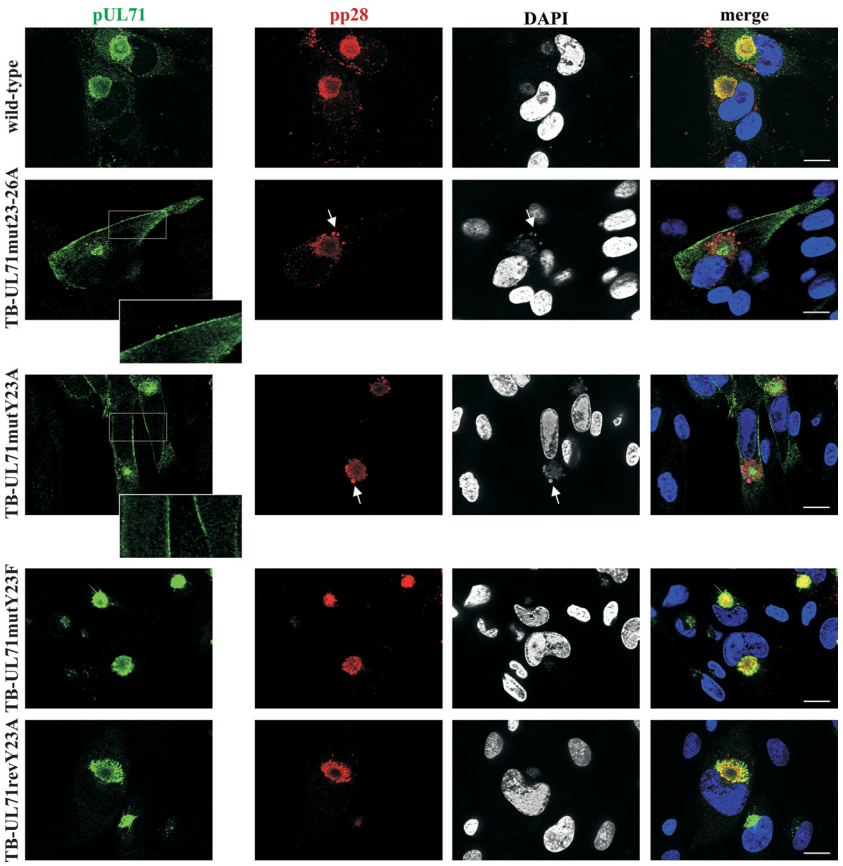

FIG 4 Subcellular localization of pUL71 and pp28 in wild-type, TB-UL71mut23–26A, TB-UL71mutY23A, TB-UL71mutY23F, and TB-UL71revY23A virus-infected HFF at 120 hpi. Proteins were detected by antibodies directed against pUL71 (green) and against pp28 (red). Cell nuclei were marked with DAPI. Arrows indicate accumulations of pp28 signals, which are also positive for DAPI, at the area of the vAC. Scale bar, 20 μm. Boxed areas of the TB-UL71mut23–26A and TB-UL71mutY23A infections are shown at higher magnification in the insets.

plasma membrane (26). Endocytosis of proteins from the plasma membrane is achieved by using different trafficking pathways, with clathrin-mediated endocytosis as the main pathway (49). Therefore, we tested whether pUL71 trafficking involves endocytosis by pharmacologically blocking this pathway. Transiently expressing HeLa cells were treated with 30 mM methyl-β-cyclodextrin (MβCD) for 45 min (Fig. 6B). MβCD causes inhibition of endocytosis by depletion of cholesterol in the plasma membrane (50, 51). Inhibition of endocytosis was verified by pulse-labeling of cells with Alexa Fluor 568-conjugated human transferrin, which is constitutively taken up into cells by the transferrin receptor, with the latter being internalized by clathrin-mediated endocytosis (52). As shown in Fig. 6B, transferrin accumulated at the plasma membrane of cells treated with MβCD, indicative of inhibition of endocytosis, while it was internalized in cells without MβCD (Fig. 6A). Plasma membrane accumulation was also observed for transiently expressed pUL71eGFP and pUL71eGFP_1–34 proteins after 45 min of incubation with MβCD (Fig. 6B), whereas these proteins exhibited TGN localization in untreated control cells. It has been reported that YXXΦ motifs can be recruited by the adaptor protein complex 2 (AP-2) of clathrin-mediated endocytosis (26). To verify our results, a more specific and less harmful way to inhibit clathrin-mediated endocytosis was chosen by coexpression of the C-terminal part of cellular AP180 (AP180-C). AP180-C specifically inhibits clathrin-mediated endocytosis by interfering with the AP180-induced formation of clathrin-coated pits (37). Coexpression of AP180-C together with either pUL71eGFP, pUL71eGFP_1–34, or pUL71eGFP_Y23F in HeLa cells caused plasma membrane accumulation of pUL71eGFP, similar to results in cells expressing only the

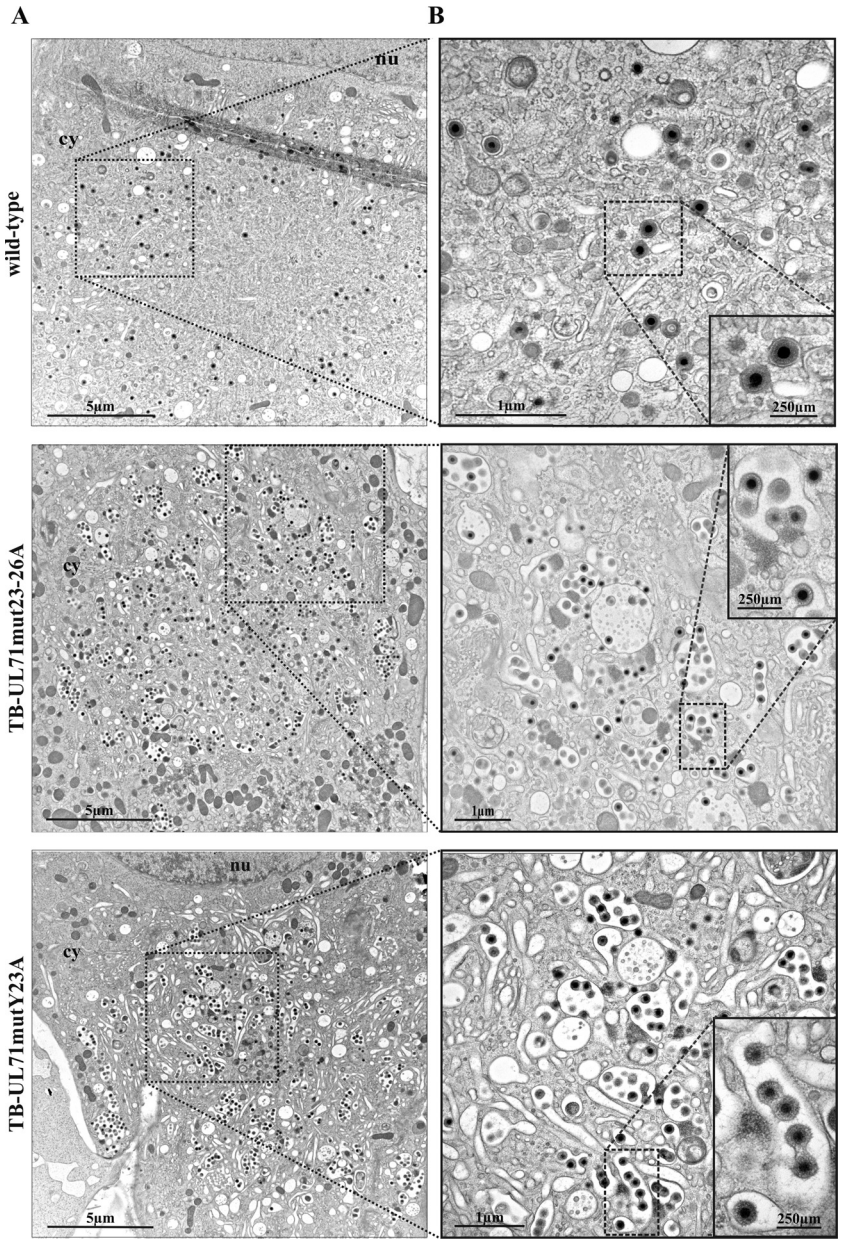

FIG 5 Ultrastructural analysis of wild-type, TB-UL71mut23–26A, and TB-UL71mutY23A virus-infected HFF at 120 hpi. (A) Electron micrographs of the area of vACs in the cytoplasm (cy) of infected cells with parts of the nucleus (nu). (B) Higher magnifications with close-ups of selected areas show fully enveloped particles for the wild-type-infected cell and multiple budding events and incompletely enveloped particles for TB-UL71mut23–26A and TB-UL71mutY23A virus-infected cells.

pUL71eGFP_Y23A mutant (Fig. 7B). In MβCD-treated cells, coexpression of AP180-C had no visible additional effect on the localization of pUL71eGFP_Y23A (Fig. 6B and 7B). Transferrin uptake, however, was visibly abrogated only in AP180-C-expressing cells (Fig. 7A), verifying block of endocytosis in those cells. Together, these results suggest a trafficking model of pUL71 in which pUL71 is delivered to the plasma membrane of transiently expressing/infected cells (Fig. 8), recruited to clathrin-coated pits via its YXXΦ motif, endocytosed, and targeted to the Golgi complex. MβCD treatment and AP180-C coexpression are able to inhibit endocytosis of pUL71 by depletion of cholesterol or by interfering with the recruitment of proteins to clathrin-coated pits.

TABLE 1 Ultrastructural quantification of secondary envelopment stages of HCMV particles in vACs of infected HFF at 120 h postinfection

Virus	No. of cells analyzed	No. of capsids per vAC	% particles by type (mean ± SD)[a]		
			Enveloped	Membrane attached	Naked
Wild type	14	27 ± 12	**57.7** ± 19.6	35.0 ± 17.4	7.2 ± 11.7
TB-UL71mut23–26	12	241 ± 147	10.9 ± 7.0	**82.6** ± 7.2	6.5 ± 7.4
TB-UL71mutY23A	10	166 ± 126	16.8 ± 12.3	**75.9** ± 10.9	7.3 ± 5.0

[a]Given are the mean percentages and standard deviations (SD) of the numbers of enveloped particles, particles attached to membranes, and nonenveloped particles not attached to membranes (naked). For each virus, boldface values highlight the stage of secondary envelopment at which the majority of particles were counted.

DISCUSSION

The tegument protein pUL71 was previously identified as a structural component of HCMV virions that in infection accumulates at the site of virion assembly, the vAC (42, 53). Absence of pUL71 during infection results in impaired secondary envelopment, leading to the accumulation of capsids at various budding stages (40, 41). These data indicate a block during secondary envelopment at the last stage of membrane scission.

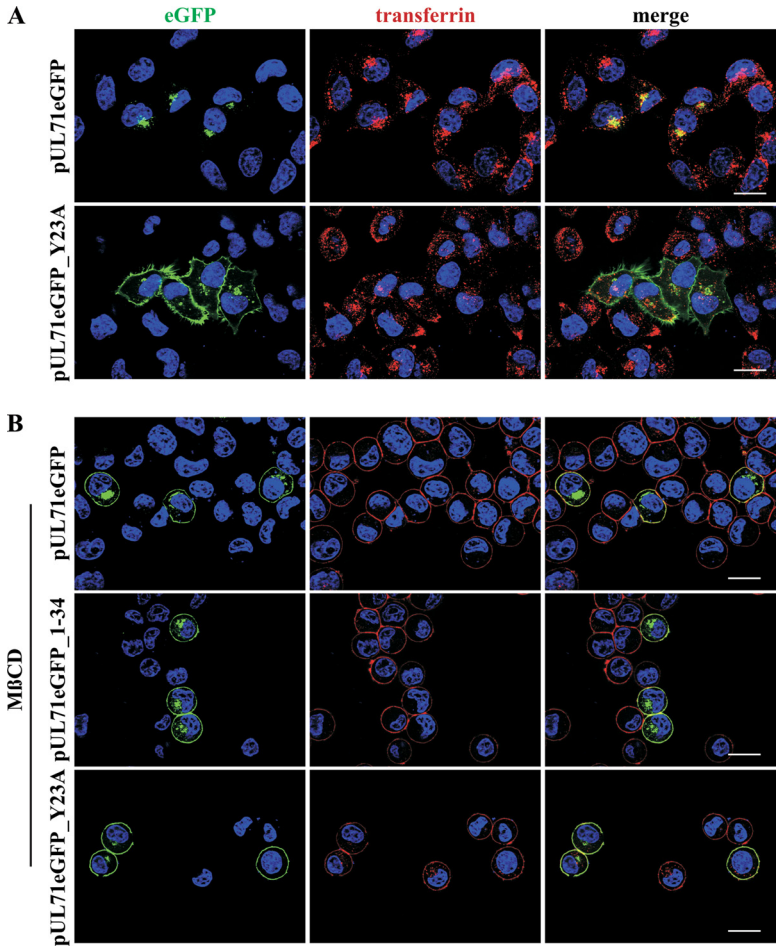

FIG 6 Inhibition of endocytosis by methyl-β-cyclodextrin (MβCD). (A) HeLa cells transiently expressing pUL71eGFP and pUL71eGFP_Y23A were incubated with 5 μg/ml human transferrin conjugated with Alexa Fluor 568 for 30 min at 37°C. Afterwards, cells were fixed, stained with DAPI, and examined using a fluorescence microscope. (B) Endocytosis of HeLa cells transiently expressing the indicated pUL71 proteins was inhibited by incubation in serum-free medium supplemented with 30 mM MβCD for 45 min. At 30 min prior to fixation, endocytosis inhibition was controlled by adding 5 μg/ml human transferrin conjugated with Alexa Fluor 568. Following fixation, cell nuclei were stained with DAPI and analyzed by fluorescence microscopy. Scale bar, 20 μm.

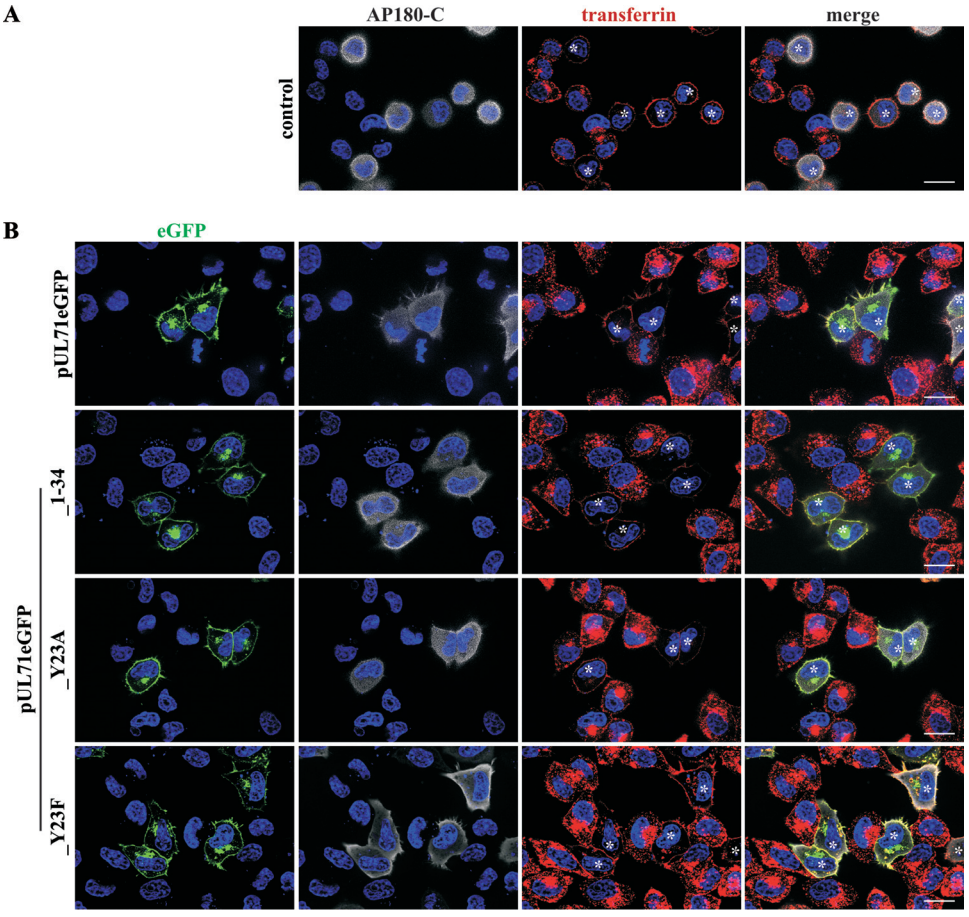

FIG 7 Inhibition of clathrin-mediated endocytosis by coexpression of AP180-C. (A) Inhibition of endocytosis in AP180-C-expressing HeLa cells was tested by transferrin uptake at 20 h posttransfection (control). After uptake of Alexa Fluor 568-conjugated human transferrin for 30 min, cells were fixed. AP180-C was detected with a primary antibody against its myc tag and a secondary antibody coupled to Alexa Fluor 647 (white). (B) HeLa cells coexpressing the indicated pUL71eGFP proteins (green) and AP180-C were tested for endocytosis inhibition as described for control cells. Cell nuclei were stained with DAPI. AP180-C-positive cells are indicated with an asterisk. Scale bar, 20 μm.

The exact function of pUL71 in this process, however, remains to be clarified. Here, we found that pUL71 requires an N-terminal YXXΦ trafficking signal for its localization at the Golgi complex in transient expression as well as for its localization at the vAC during infection. Most importantly, mutation of the YXXΦ motif resulted in delocalization of mutated pUL71 and in impaired infectious virus release as well as in defective spread of TB-UL71mut23–26A and TB-UL71mutY23A viruses that was similar to the spread defect of a UL71-deficient virus (40). The observed growth and spread defect can be explained by the impaired secondary envelopment of virus particles in YXXΦ mutant virus infections, as demonstrated by ultrastructural analysis. These data show that the localization of pUL71 at the vAC is critical for its function during virus morphogenesis. They also emphasize the proposed function of pUL71 for secondary envelopment and show the importance of the vAC as the primary site of this process. Mutations of the viral genome are prone to unwanted effects on either neighboring genes or functional domains. The point mutant TB-UL71mutY23A is a mutant with minimal changes to the wild-type virus sequence. This mutant, as well as the mutant with the entire YXXΦ motif mutated, exhibited identical phenotypes in localization studies, growth analysis, and ultrastructural analysis, indicating a specific effect caused by disruption of the YXXΦ motif. However, we cannot entirely exclude that other potential roles of the tyrosine that may be critical for proper function of pUL71 in infection may be disrupted by

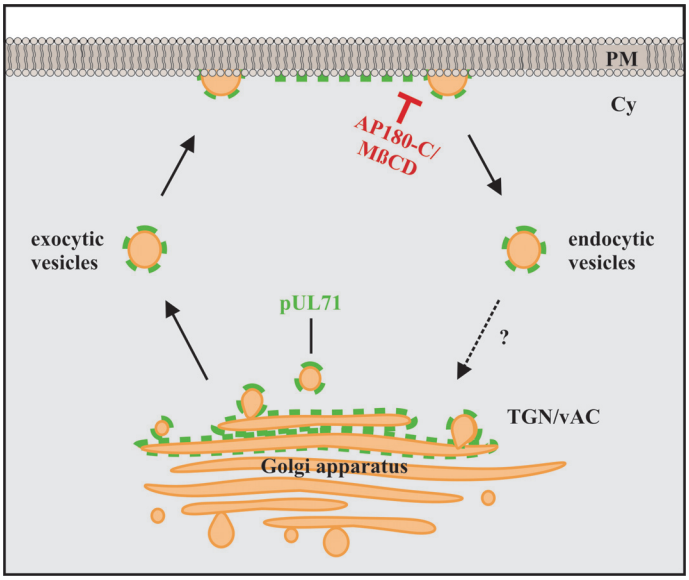

FIG 8 Model of intracellular trafficking of pUL71 in transfected and infected cells. Indicated is a potential trafficking route from the Golgi apparatus, delivering membrane-associated pUL71 to the plasma membrane (PM). At the plasma membrane, where pUL71 is localized at the cytosolic phase, recognition of the N-terminal YXXΦ motif recruits pUL71 to endocytic vesicles; pUL71 then gets recycled back by yet unknown mechanisms (question mark) to the Golgi apparatus or vAC in infection. Endocytosis from the plasma membrane can be blocked by coexpression of AP180-C and cholesterol depletion using methyl-β-cyclodextrin (MβCD). Cy, cytoplasm.

substitution of an alanine. One potential role could be phosphorylation since tyrosines are known to serve as phosphorylation sites (54). The successful exchange of tyrosine for the very similar phenylalanine, however, argues against an important role of phosphorylation. The substitution in mutant TB-UL71mutY23F rescued not only localization of pUL71 to the vAC but also viral growth, supporting the importance of the localization of pUL71 for its function during assembly and egress.

Several lines of evidence indicate that the pUL71 YXXΦ motif is indeed involved in retrieval of pUL71 from the plasma membrane by endocytosis. Thus, pUL71 accumulated at the plasma membrane when this motif was mutated. Moreover, pharmacological inhibition of endocytosis and expression of a transdominant negative inhibitor of clathrin-mediated endocytosis prevented recycling of pUL71. In both cases of endocytosis inhibition, cholesterol depletion by MβCD and expression of AP180-C, wild-type pUL71 accumulated at the plasma membrane at levels similar to those of the pUL71eGFP_Y23A and pUL71eGFP_1–22 proteins. Cholesterol depletion by MβCD is known to block endocytosis at the very initial step before endocytic vesicles are formed (51). Consistent with the inhibition of endocytosis by cholesterol depletion, uptake of transferrin was blocked. Transferrin uptake is commonly used to control for endocytosis (51, 55). While cholesterol depletion is a relatively unspecific method, it can be used to temporarily block endocytosis, which is an indication for rapid intracellular trafficking of pUL71. Trafficking signals, such as the YXXΦ motif, are recognized at the plasma membrane by the μ2 subunit of the AP-2 complex, which mediates clathrin-dependent endocytosis by interaction of the AP-2 complex with AP180 and clathrin (37). Because of the central role of AP180 in initiating clathrin-dependent endocytosis, overexpression of the AP180-C terminus specifically inhibits this endocytic pathway (49). Therefore, plasma membrane accumulation of wild-type pUL71 in AP180-C-expressing cells argues for the utilization of the clathrin-dependent endocytosis pathway to retrieve pUL71 from the plasma membrane.

There is strong evidence that endocytosis plays important roles for the virus life cycle of many viruses, including HCMV (22, 56–58). This is highlighted by the finding that many viral proteins, primarily glycoproteins of HCMV and other viruses, are known

to carry trafficking signals, including YXXΦ motifs (13–22, 56, 59). The importance of these signals has been analyzed in many cases. Mutation of such trafficking signals, e.g., in HCMV gpUL132 (14), results in accumulation of gpUL132 at the plasma membrane in infection, similarly to what is shown in this study for pUL71 in YXXΦ mutant virus infection. In contrast to studies of glycoproteins, which have a transmembrane domain for membrane anchoring, relatively few studies of endocytosis have been carried out with proteins peripherally associated with the cytoplasmic side of membranes. HCMV tegument proteins, including pUL71, lack a transmembrane domain through which they interact with membranes. Membrane association of such proteins can be facilitated via a lipid anchor. One example of clathrin-mediated endocytosis from the plasma membrane of a membrane-associated protein is the vaccinia virus (VV) F13L protein (57, 60). VV F13L accumulates at the plasma membrane when clathrin-mediated endocytosis is inhibited by drugs or expression of transdominant negative inhibitors of endocytosis (60, 61). Membrane association of VV F13L is facilitated by palmitoylation (62). Palmitoylation of HCMV pUL71 has yet to be shown. However, the pUL51 protein of HSV-1, a functional homologue of HCMV pUL71, has been shown to be palmitoylated at the N terminus (38). In addition, palmitoylation of HSV-1 pUL51 is required for its Golgi complex association. Palmitoylation appears to be conserved among pUL71 homologues as potential palmitoylation sites can be found in their sequences (45). Furthermore, N-terminal amino acids 1 to 34 of pUL71 are sufficient to locate eGFP at the Golgi compartment. This sequence of pUL71 contains both potential palmitoylation sites and the YXXΦ trafficking signal. In addition to a similar intracellular localization, functional homology has also been reported for HSV-1 pUL51 (44) as well as for the VV F13L protein (61). The latter has been suggested to induce formation of vesicles that contain other viral envelope proteins and are precursors of the wrapping membranes in VV infection, which is reminiscent to what is known as secondary envelopment in herpesviruses (60). The YXXΦ trafficking signal near the N terminus of pUL71 can be found in sequences of pUL71 homologues of other herpesviruses (45). In contrast to HCMV pUL71, mutation of this motif in HSV-1 pUL51 has very little effect on virus replication and release but causes a cell-type-specific defect in cell-to-cell spread (45). The reason for this difference between HCMV and HSV is not clear, but it is not known whether mutation of the YXXΦ motif in HSV-1 pUL51 alters intracellular localization of this protein, as shown for HCMV pUL71 in this study. To our knowledge, the role of the YXXΦ trafficking signal for endocytosis of pUL71 homologues has not been investigated in other herpesviruses. Endocytosis of HCMV pUL71 may allow the retrieval and reuse of this protein for the process of secondary envelopment. The challenge for herpesviruses is the temporal and spatial coordination of the many viral structural proteins that need to be incorporated into virions. Different intracellular trafficking mechanisms have already been shown to be used by different HCMV-encoded proteins for their accumulation at the vAC (12, 58). In addition, the use of the same intracellular trafficking pathways by several viral proteins may represent a possible mechanism to concentrate these proteins at the site of secondary envelopment. Based on previous data on homologous proteins and our data, we propose the following intracellular trafficking scheme for HCMV pUL71: it is expressed as a cytosolic protein and associates with Golgi complex-derived membranes (Fig. 8). It reaches the plasma membrane as a result of trafficking via the secretory pathway either with virion-containing vesicles or exocytic vesicles derived from the TGN. Recognition of the YXXΦ motif of pUL71 at the plasma membrane induces endocytosis via clathrin-coated vesicles. Upon internalization from the plasma membrane, these vesicles fuse with early/sorting endosomes, eventually reaching the endocytic recycling compartment (ERC). At the ERC, proteins can be sorted to the TGN. Protein trafficking between secretory cellular compartments is organized by the adaptor protein complex 1 (AP-1) and other adaptors as family members of the phosphofurin acidic cluster sorting (PACS) proteins. For HCMV gB, ERC-to-Golgi complex trafficking is executed by PACS-1 (17). The adaptor protein by which pUL71 is targeted to the Golgi compartment is currently not known. However, the presence of negatively charged amino acids within the N-terminal fragment of 34

amino acids could indicate PACS-1-mediated sorting, which has to be shown in future studies.

Together, the data from this study show that herpesvirus tegument proteins hijack clathrin-mediated endocytosis for their intracellular trafficking to the virion assembly site. The importance of this trafficking for the generation of infectious virus particles opens the possibility of interfering with such a pathway in order to inhibit viral growth.

MATERIALS AND METHODS

Cell culture. Human foreskin fibroblasts (HFF) and human fetal lung cells (MRC-5; European Collection of Cell Cultures) were maintained in minimal essential medium (Gibco-BRL) supplemented with 2 mM L-glutamine. HeLa cells were maintained in Dulbecco's modified Eagle medium (DMEM; Gibco-BRL). All cell culture media were supplemented with 10% fetal calf serum, 1× nonessential amino acids (both from Biochrom AG), 100 U of penicillin, and 100 μg of streptomycin (both from Gibco-BRL).

Expression plasmids and transient protein expression. To construct pEF-UL71eGFP-expressing full-length pUL71 fused to eGFP, the UL71eGFP fragment was amplified from the bacmid pTB-UL71eGFP with the primers ex-UL71_for (5′-TACGGGATCCATGCAGCTGGCCCAGCGC-3′) and ex-UL71_rev (5′-TACGGAATTCTTTTCCAAAACGTGCCAGGCTGT-3′) and cloned into the StrataClone vector (pSC-B; Stratagene). The UL71eGFP fragment was released from pSC-B-UL71eGFP and inserted into pEF1/Myc-His C (Invitrogen) by using EcoRI. Plasmid pEF-UL71eGFP_1–34 expressing pUL71 amino acids 1 to 34 fused to eGFP was constructed by first amplifying the fragments UL71_1–34 (ex-UL71_for, 5′-TACGGGATCCATGCAGCTGGCCCAGCGC-3′; ex-UL71_1–34_rev, 5′-CAGGATCCCTCCACGTCCTCGCTAGGCTG-3′) and eGFP (ex-BglII+EGFP/ATG_for, 5′-CTAGATCTGTGAGCAAGGGCGAGGAGCTG-3′; eGFP-EcoRI_rev, 5′-GATGAATTCGCGGCCGCTTTACTTGTACAGCTC-3′) from pEF-UL71eGFP. UL71eGFP_1–34 was amplified with the primers ex-UL71_for and eGFP-EcoRI_rev after ligation of these fragments via BamHI and BglII and cloned into pEF1/Myc-His C using BamHI and EcoRI. To construct pEF-UL71eGFP_1–22, the sequence of pUL71 amino acids 1 to 22 was added to the sequence of eGFP by PCR using the primers ex-UL71eGFP_1–22_for (5′-TCGGATCCATGCAGCTGGCCCAGCGCCTGTGCGAGCTGCTGATGTGCCGTCGCAAAGCCGCGCCTGTGGCCGATGGATCTGTGAGCAAGGGCGAGG-3′) and ex-eGFP_rev (5′-TGACGCGGCCGCTTACTTGTACAGCTCGTCCATGCCG-3′). The fragment UL71eGFP_1–22 was first cloned into the pCR2.1-TOPO TA Vector (Thermo Fisher) before being cloning into pEF1/Myc-His C using BamHI and EcoRI. Plasmid pEF-UL71eGFP_Y23A was constructed implementing site-directed mutagenesis by amplification of pEF-UL71eGFP with sdm-UL71Y23A_for (5′-TGTGGCCGATGCCGTGCTGCTG-3′) and sdm-UL71Y23A_rev (5′-CAGCAGCACGGCATCGGCCACA-3′). Expression plasmids pEF-UL71eGFP_23–26A and pEF-UL71eGFP_Y23F were constructed on the basis of plasmid pEF-UL71eGFP by using a Gibson assembly cloning kit (New England BioLabs). The backbone and insert for Gibson assembly of pEF-UL71eGFP_23–26A were amplified by PCR using the primers ga-pEF-after NotI_for (5′-TCGAGGTCACCCATTCGAAC-3′) and ga-UL71_23–26AeGFP_rev (5′-TGAGCGGCAGCGGCATCGGCCACAGGCGCGGC-3′) for amplification of the backbone and the primers ga-UL71_23–26AeGFP_for (5′-TGTGGCCGATGCCGCTGCCGCTCAGCCTAGCGAGGACGTG-3′) and ga-pEF-UL71_eGFP_rev (5′-GTTCGAATGGGTGACCTCGAGCGGCCGCTTACTTGTAC-3′) for amplification of the insert. For cloning of plasmid pEF-UL71eGFP_Y23F, the backbone was amplified by PCR using the primers ga-pEF-after NotI_for (5′-TCGAGGTCACCCATTCGAAC-3′) and ga-pEF-UL71_rev (5′-AATCGGCCACAGGCGCGG-3′), and the insert was amplified by using the primers ga-pEF-UL71_Y23F_for (5′-AGCCGCGCCTGTGGCCGATTTCGTGCTGCTGCAGCCTAGC-3′) and ga-pEF-UL71_eGFP_rev (5′-GTTCGAATGGGTGACCTCGAGCGGCCGCTTACTTGTAC-3′). All cloning was performed in *Escherichia coli* strain XL1-Blue. The generation of the expression plasmid that was used to express a myc epitope-tagged AP180-C is described elsewhere (37). For transient expression experiments, HeLa cells were seeded on coverslips in 24-well plates and transfected the next day by using TurboFect (Thermo Fisher) according to the manufacturer's protocol. For indirect immunostaining, cells were fixed with 4% paraformaldehyde (PFA) in phosphate-buffered saline (PBS) for 10 min at 4°C at 20 h posttransfection. Indirect immunostaining was performed as described for infected cells with an altered blocking buffer (5% fetal calf serum [FCS] in PBS supplemented with 1% bovine serum albumin [BSA]).

Generation of recombinant viruses. Recombinant viruses were reconstituted from recombinant bacterial artificial chromosomes (BACs) generated on the genetic background of the TB40-BAC4 BAC (GenBank accession number EF999921.1) (63). All BAC mutants were generated by using a markerless two-step Red-GAM recombination protocol (64). For virus reconstitution, BAC DNA was extracted from *E. coli* using a Nucleobond AX Midi kit (Macherey-Nagel) and electroporated into MRC-5 cells exactly as previously described (65). For further virus propagation and stock production, HFF were used. The parental BAC of all recombinant BAC mutants of this study contains the sequence of the Flag tag epitope at the end of UL103 and was constructed using the primers ep-UL103-Flag_for (5′-CCCCAAGCTGCCACCGCGCTGGGAACGGGGAGAGGAAGAGGATTACAAGGATGACGACGATAAGTGAGAAGCAGGATGACGACGATAAGTAGGG-3′) and ep-UL103-Flag_rev (5′-GTTTTTTTTTCTATGATATGCGTGTCTAGTTCGCTTCTCACTTATCGTCGTCATCCTTGTAATCCTCTTCCTCAACCAATTAACCAATTCTGATTAG-3′). The resulting reconstituted virus was designated the wild-type virus in this study. The primers ep-UL71YXXL_for (5′-TGATGTGCCGTCGCAAAGCCGCGCCTGTGGCCGATGCCGCTGCCGCTCAGCCTAGCGAGGAGATGACGACGATAAGTAGGG-3′) and ep-UL71YXXL_rev (5′-TGCAGCTCGCGCAGCTCCACGTCCTCGCTAGGCTGAGCGGCAGCGGCATCGGCCACAGGCGAATTAACCAATTCTGATTAG-3′) were used to generate the bacmid of the mutant virus TB-UL71mutY23–26A. The bacmid for mutant virus TB-UL71mutY23A was generated using ep-UL71Y23A_for (5′-TGATGTGCCGTCGCAAAGCCGCGCCTGTGGCCGATGCCGTGCTGCTGCAGCCTAGCGAGGAGATGACGACGATAAGTAGGG-3′) and ep-UL71Y23A_rev (5′-CGCAGCTCCACGTCCTCGCTAGGCTGCAGCAGCACGGCATCGGCCACAGGCGAATTAACCA

ATTCTGATTAG-3′). The primers ep-UL71-Y23F_for (5′-CTGCTGATGTGCCGTCGCAAAGCCGCGCCTGTGGCCGA TTTCGTGCTGCTGCAGCCTAGCGAGGATGACGACGATAAGTAGGG-3′) and ep-UL71-Y23F_rev (5′-CTCGCGCAGC TCCACGTCCTCGCTAGGCTGCAGCAGCACGAAATCGGCCACAGGCGCGGCTCAACCAATTAACCAATTCTGATTAG-3′) were used to generate the bacmid of the mutant virus TB-UL71mutY23F. The bacmid of revertant virus TB-UL71revY23A was generated from the bacmid of point mutant TB-UL71mutY23A by using ep-UL71-23Aresc_for (5′-GCTGCTGATGTGCCGTCGCAAAGCCGCGCCTGTGGCCGATTATGTGCTGCTGCAGC CTAGCGAGGACAGGATGACGACGATAAGTAGGG-3′) and ep-UL71-23Aresc_rev (5′-ACGCCTGCAGCTCG-CGCAGCTCCACGTCCTCGCTAGGCTGCAGCAGCACATAATCGGCCACAGGCGCCAACCAATTAACCAATTCTGA TTAG-3′). In order to discriminate between wild-type and revertant viruses, a silent mutation was introduced into TB-UL71revY23A. Correct introduction of all mutations into the recombinant BACs was confirmed by sequencing. The generation and characterization of mutant virus TB-UL71stop unable to express pUL71 are described elsewhere (40).

Antibodies. The monoclonal antibody (MAb) used in indirect immunofluorescence stainings is directed against the HCMV protein pp28 (UL99, clone CH19; Santa Cruz). Additionally, anti-myc tag antibody (MAb 9E10) was used to detect AP180-C. The polyclonal antibodies (PAbs) used in this study are directed against HCMV pUL71 (PAb consisting of residues 162 to 361 [40]) and against cellular Golgi complex protein TGN46 (catalog no. T7576; Sigma). Goat anti-rabbit and goat anti-mouse antibodies conjugated to either Alexa Fluor 488, 555, or 647 (Thermo Fisher) were used as secondary antibodies.

Indirect immunofluorescence. For virus infection, HFF were seeded at 80% confluence 1 day prior to infection on μ-Slides (Ibidi GmbH). The following day, cells were infected at a multiplicity of infection (MOI) between 0.5 and 1. At 120 hpi, cells were washed once with PBS prior to fixation with 4% PFA in PBS for 10 min at 4°C. After being washed with PBS, cells were permeabilized with 0.1% Triton in PBS for 5 min at room temperature. Nonspecific binding sites were blocked by incubation in blocking buffer (10% CMV-negative human serum and 1% bovine serum albumin [BSA] in PBS) for 30 min. Primary as well as secondary antibodies were diluted in blocking buffer. Following blocking, cells were incubated with primary antibody for at least 45 min before being washed three times with washing solution (1% BSA in PBS with 0.1% Tween 20) and incubation with secondary antibody for 45 min. Cell nuclei were stained with 30 μg/ml 4,6-diamidino-2-phenylindole (DAPI; Roche) together with the secondary antibody. Cells were washed three times with PBS prior to imaging. If not stated otherwise, confocal images were taken with a 63×objective lens of an Axio-Observer.Z1 fluorescence microscope equipped with an ApoTome (Zeiss) and Axiovision, version 4.8, software.

Growth analysis and virus titration. A multistep growth kinetics analysis was performed by coseeding of noninfected HFF with infected HFF at 1 dpi. Coseeding was performed in quadruplicate. Equal infection was controlled by detection of HCMV IE1/2 antigen in indirect immunofluorescence of one replicate 24 h after coseeding to determine input virus yields by counting IE-positive cells. Supernatants of infected cells were collected over a period of 15 days every 3 days and replaced with fresh medium. All supernatants were stored at −80°C before titration on HFF. Virus yield in supernatant was determined by infecting HFF with 10-fold serial dilutions of supernatant. At 24 hpi infected cells were fixed and permeabilized with ice-cold methanol and stained by indirect immunostaining against HCMV IE1/2 antigen. IE1/2-positive cells were counted by using a 10× objective lens on an Axio-Observer.Z1 fluorescence microscope. For the focus expansion assay, HFF were infected with 100 PFU of the respective viruses for 24 h. Inoculum was removed and replaced with 0.65% methylcellulose overlay medium, which was exchanged with fresh overlay medium at 4 dpi. At 7 dpi, overlay medium was removed by washing cells with PBS, followed by fixation with ice-cold methanol for 10 min. Foci of virus-infected cells were visualized by indirect immunostaining against the HCMV IE1/2 antigen. Numbers of IE1/2-positive cells/focus were determined for 50 foci for each virus. Randomly taken images were acquired with the 10× objective lens of an Axio-Observer.Z1 fluorescence microscope and the Axiovision, version 4.8, software and analyzed with Adobe Photoshop CS3 software. Statistical significance was determined with a two-tailed Student's *t* test.

TEM. Sample preparation for transmission electron microscopy (TEM) included high-pressure freezing (HPF), freeze substitution, and Epon embedding. These methods were performed as previously described (41, 66), with slight alterations. Briefly, HFF were seeded in μ-Slides containing carbon-coated sapphire discs (Engineering Office M. Wohlwend GmbH) 1 day prior to infection at 80 to 90% confluence. Cells were infected with virus overnight, resulting in an infection rate of 40 to 60%. Virus-containing medium was replaced with fresh medium the next day. Infected cells on sapphire discs were fixed by using HPF with a Compact 01 high-pressure freezer (Engineering Office M. Wohlwend GmbH) at 120 hpi. Thereafter, cells on sapphire discs were prepared by freeze-substitution (66, 67) and subsequently embedded in Epon (Fluka). Ultrathin sections of the Epon-embedded cells were cut with an ultramicrotome (Ultracut UCT; Leica) and placed on Formvar-coated single-slot grids (Plano GmbH). Grids were examined in a Jeol JEM-1400 transmission electron microscope equipped with a charge-coupled-device (CCD) camera at an acceleration voltage of 120 kV. The remaining cells in the μ-Slide were fixed with 4% PFA in PBS for 10 min at 4°C. They were used in indirect immunofluorescence staining to control infection rates and mutant virus characteristics.

Quantification of secondary envelopment by TEM. Virus particles in the area of the vAC were quantified from electron micrographs of infected cells at 120 hpi (68). Virus particles were divided into three groups according to their morphological stages of secondary envelopment (41). Enveloped virus particles are capsids with tegument fully enclosed by a double membrane (envelope and vesicle membrane). Membrane-attached capsids are capsids at the process of secondary envelopment, which was defined as close contact to membranes which wrap around the capsid. Free capsids are those that have no contact with membranes. Infected cells for quantification were randomly selected from at least

two independent experiments. For each analyzed vAC, magnified electron micrographs covering the entire area of the vAC were acquired to determine the various stages of secondary envelopment of virus particles.

Cholesterol depletion and transferrin uptake. Transiently expressing HeLa cells were washed with PBS and incubated at 37°C in either serum-free DMEM or serum-free DMEM supplemented with 30 mM methyl-β-cyclodextrin (MβCD; Sigma) to deplete cholesterol. After 15 min of incubation, transferrin uptake was assessed by adding 5 μg/ml of Alexa Fluor 568-conjugated human transferrin (Invitrogen) and incubation for an additional 30 min at 37°C (55). Afterwards, cells were washed with PBS and fixed with 4% PFA in PBS.

ACKNOWLEDGMENTS

The technical assistance of Anke Lüske is gratefully acknowledged. We thank Paul Walther (Central Facility for Electron Microscopy, Ulm, Germany) and Lukas Wettstein, Sina Lippold, Marco Castelli, and Christian Sinzger (Institute of Virology, Ulm, Germany) for their experimental help.

This work was supported by the MWK Baden-Wuerttemberg through the Junior Professor Program.

REFERENCES

1. Griffiths PD. 2012. Burden of disease associated with human cytomegalovirus and prospects for elimination by universal immunisation. Lancet Infect Dis 12:790–798. https://doi.org/10.1016/S1473-3099(12)70197-4.
2. Mocarski ES, Shenk T, Pass RF. 2007. Cytomegaloviruses, p 2701–2772. *In* Knipe DM, Howley PM, Griffin DE, Lamb RA, Martin MA, Roizman B, Straus SE (ed), Fields virology, 5th ed, vol 2. Lippincott Williams & Wilkins, Philadelphia, PA.
3. Baldick CJ, Shenk T. 1996. Functional analysis of the pseudorabies virus UL51 protein. J Virol 70:6097–6105.
4. Varnum SM, Streblow DN, Monroe ME, Smith P, Auberry KJ, Pasa-Tolic L, Wang D, Camp DG, II, Rodland K, Wiley S, Britt W, Shenk T, Smith RD, Jay A, Pas L, Nelson JA. 2004. Identification of proteins in human cytomegalovirus (HCMV) particles: the HCMV proteome. J Virol 78:10960–10966. https://doi.org/10.1128/JVI.78.20.10960-10966.2004.
5. Terhune SS, Schröer J, Shenk T. 2004. RNAs are packaged into human cytomegalovirus virions in proportion to their intracellular concentration. J Virol 78:10390–10398. https://doi.org/10.1128/JVI.78.19.10390-10398.2004.
6. Mettenleiter TC, Klupp BG, Granzow H. 2006. Herpesvirus assembly: a tale of two membranes. Curr Opin Microbiol 9:423–429. https://doi.org/10.1016/j.mib.2006.06.013.
7. Mettenleiter TC, Klupp BG, Granzow H. 2009. Herpesvirus assembly: an update. Virus Res 143:222–234. https://doi.org/10.1016/j.virusres.2009.03.018.
8. Sanchez V, Greis KD, Sztul E, Britt WJ. 2000. Accumulation of virion tegument and envelope proteins in a stable cytoplasmic compartment during human cytomegalovirus replication: characterization of a potential site of virus assembly. J Virol 74:975–986. https://doi.org/10.1128/JVI.74.2.975-986.2000.
9. Cepeda V, Esteban M, Fraile-Ramos A. 2010. Human cytomegalovirus final envelopment on membranes containing both trans-Golgi network and endosomal markers. Cell Microbiol 12:386–404. https://doi.org/10.1111/j.1462-5822.2009.01405.x.
10. Das S, Vasanji A, Pellett PE. 2007. Three-dimensional structure of the human cytomegalovirus cytoplasmic virion assembly complex includes a reoriented secretory apparatus. J Virol 81:11861–11869. https://doi.org/10.1128/JVI.01077-07.
11. Dunn W, Chou C, Li H, Hai R, Patterson D, Stolc V, Zhu H, Liu F. 2003. Functional profiling of a human cytomegalovirus genome. Proc Natl Acad Sci U S A 100:14223–14228. https://doi.org/10.1073/pnas.2334032100.
12. Moorman NJ, Sharon-Friling R, Shenk T, Cristea IM. 2010. A targeted spatial-temporal proteomics approach implicates multiple cellular trafficking pathways in human cytomegalovirus virion maturation. Mol Cell Proteomics 9:851–860. https://doi.org/10.1074/mcp.M900485-MCP200.
13. Pasieka TJ, Maresova L, Grose C. 2003. A functional YNKI motif in the short cytoplasmic tail of varicella-zoster virus glycoprotein gH mediates clathrin-dependent and antibody-independent endocytosis. J Virol 77:4191–4204. https://doi.org/10.1128/JVI.77.7.4191-4204.2003.
14. Kropff B, Koedel Y, Britt W, Mach M. 2010. Optimal replication of human cytomegalovirus correlates with endocytosis of glycoprotein gpUL132. J Virol 84:7039–7052. https://doi.org/10.1128/JVI.01644-09.
15. Sanchez V, Sztul E, Britt WJ. 2000. Human cytomegalovirus pp28 (UL99) localizes to a cytoplasmic compartment which overlaps the endoplasmic reticulum-Golgi-intermediate compartment. J Virol 74:3842–3851. https://doi.org/10.1128/JVI.74.8.3842-3851.2000.
16. Olson JK, Grose C. 1997. Endocytosis and recycling of varicella-zoster virus Fc receptor glycoprotein gE: internalization mediated by a YXXL motif in the cytoplasmic tail. J Virol 71:4042–4054.
17. Crump CM, Hung C-H, Thomas L, Wan L, Thomas G. 2003. Role of PACS-1 in trafficking of human cytomegalovirus glycoprotein B and virus production. J Virol 77:11105–11113. https://doi.org/10.1128/JVI.77.20.11105-11113.2003.
18. Foster TP, Melancon JM, Olivier TL, Kousoulas KG. 2004. Herpes simplex virus type 1 glycoprotein K and the UL20 protein are Interdependent for intracellular trafficking and trans-Golgi network localization. J Virol 78:13262–13277. https://doi.org/10.1128/JVI.78.23.13262-13277.2004.
19. Tirabassi RS, Enquist LW. 1999. Mutation of the YXXL endocytosis motif in the cytoplasmic tail of pseudorabies virus gE. J Virol 73:2717–2728.
20. Mach M, Osinski K, Kropff B, Schloetzer-Schrehardt U, Krzyzaniak M, Britt W. 2007. The carboxy-terminal domain of glycoprotein N of human cytomegalovirus is required for virion morphogenesis. J Virol 81:5212–5224. https://doi.org/10.1128/JVI.01463-06.
21. Heineman TC, Hall SL. 2001. VZV gB endocytosis and Golgi localization are mediated by YXXphi motifs in its cytoplasmic domain. Virology 285:42–49. https://doi.org/10.1006/viro.2001.0930.
22. Albecka A, Laine RF, Janssen AFJ, Kaminski CF, Crump CM. 2016. HSV-1 glycoproteins are delivered to virus assembly sites through dynamin-dependent endocytosis. Traffic 17:21–39. https://doi.org/10.1111/tra.12340.
23. Pandey Kailash N. 2009. Functional roles of short sequence motifs in the endocytosis of membrane receptors. Front Biosci 14:5339–5360. https://doi.org/10.2741/3599.
24. Collawn JF, Stangel M, Kuhn LA, Esekogwu V, Jing S, Trowbridge IS, Tainer JA. 1990. Transferrin receptor internalization sequence YXRF implicates a tight turn as the structural recognition motif for endocytosis. Cell 63:1061–1072. https://doi.org/10.1016/0092-8674(90)90509-D.
25. Jadot M, Canfield WM, Gregory W, Kornfeld S. 1992. Characterization of the signal for rapid internalization of the bovine mannose 6-phosphate/insulin-like growth factor-II receptor. J Biol Chem 267:11069–11077.
26. Ohno H, Stewart J, Fournier MC, Bosshart H, Rhee I, Miyatake S, Saito T, Gallusser A, Kirchhausen T, Bonifacino JS. 1995. Interaction of tyrosine-based sorting signals with clathrin-associated proteins. Science 269:1872–1875. https://doi.org/10.1126/science.7569928.
27. Owen DJ, Evans PR. 1998. A Structural explanation for the recognition of tyrosine-based endocytotic signals. Science 282:1327–1332. https://doi.org/10.1126/science.282.5392.1327.
28. Trowbridge IS, Collawn JF, Hopkins CR. 1993. Signal-dependent membrane protein trafficking in the endocytic pathway. Annu Rev Cell Biol 9:129–161. https://doi.org/10.1146/annurev.cb.09.110193.001021.

29. Marks MS, Roche PA, Van Donselaar E, Woodruff L, Peters PJ, Bonifacino JS. 1995. A lysosomal targeting signal in the cytoplasmic tail of the β chain directs HLA-DM to MHC class II compartments. J Cell Biol 131:351–369. https://doi.org/10.1083/jcb.131.2.351.
30. Sandoval IV, Bakke O. 1994. Targeting of membrane proteins to endosomes and lysosomes. Trends Cell Biol 4:292–297. https://doi.org/10.1016/0962-8924(94)90220-8.
31. Marks MS, Woodruff L, Ohno H, Bonifacino JS. 1996. Protein targeting by tyrosine- and di-leucine-based signals: evidence for distinct saturable components. J Cell Biol 135:341–354. https://doi.org/10.1083/jcb.135.2.341.
32. Jackson MR, Nilsson T, Peterson PA. 1993. Retrieval of transmembrane proteins to the endoplasmic reticulum. J Cell Biol 121:317–333. https://doi.org/10.1083/jcb.121.2.317.
33. Matter K, Mellman I. 1994. Mechanisms of cell polarity: in epithelial cells. Curr Opin Cell Biol 6:545–554. https://doi.org/10.1016/0955-0674(94)90075-2.
34. Humphrey JS, Peters PJ, Yuan LC, Bonifacino JS. 1993. Localization of TGN38 to the trans-Golgi network: involvement of a cytoplasmic tyrosine-containing sequence. J Cell Biol 120:1123–1136. https://doi.org/10.1083/jcb.120.5.1123.
35. Ponnambalam S, Rabouille C, Luzio JP, Nilsson T, Warren G. 1994. The TGN38 glycoprotein contains two non-overlapping signals that mediate localization to the trans-Golgi network. J Cell Biol 125:253–268. https://doi.org/10.1083/jcb.125.2.253.
36. Bos K, Wraight C, Stanley KK. 1993. TGN38 is maintained in the trans-Golgi network by a tyrosine-containing motif in the cytoplasmic domain. EMBO J 12:2219–2228.
37. Ford MGJ, Pearse BMF, Higgins MK, Vallis Y, Owen DJ, Gibson A, Hopkins CR, Evans PR, McMahon HT. 2001. Simultaneous binding of PtdIns(4,5)P2 and clathrin by AP180 in the nucleation of clathrin lattices on membranes. Science 291:1051–1055. https://doi.org/10.1126/science.291.5506.1051.
38. Nozawa N, Daikoku T, Koshizuka T, Yamauchi Y, Yoshikawa T, Nishiyama Y. 2003. Subcellular localization of herpes simplex virus type 1 UL51 protein and role of palmitoylation in Golgi apparatus targeting. J Virol 77:3204–3216. https://doi.org/10.1128/JVI.77.5.3204-3216.2003.
39. Loomis JS, Bowzard JB, Courtney RJ, Wills JW. 2001. Intracellular trafficking of the UL11 tegument protein of herpes simplex virus type 1. J Virol 75:12209–12219. https://doi.org/10.1128/JVI.75.24.12209-12219.2001.
40. Schauflinger M, Fischer D, Schreiber A, Chevillotte M, Walther P, Mertens T, von Einem J. 2011. The tegument protein UL71 of human cytomegalovirus is involved in late envelopment and affects multivesicular bodies. J Virol 85:3821–3832. https://doi.org/10.1128/JVI.01540-10.
41. Schauflinger M, Villinger C, Mertens T, Walther P, von Einem J. 2013. Analysis of human cytomegalovirus secondary envelopment by advanced electron microscopy. Cell Microbiol 15:305–314. https://doi.org/10.1111/cmi.12077.
42. Womack A, Shenk T. 2010. Human cytomegalovirus tegument protein pUL71 is required for efficient virion egress. mBio 1:e00282–10. https://doi.org/10.1128/mBio.00282-10.
43. Klupp BG, Granzow H, Klopfleisch R, Fuchs W, Kopp M, Lenk M, Mettenleiter TC. 2005. Functional analysis of the pseudorabies virus UL51 protein. J Virol 79:3831–3840. https://doi.org/10.1128/JVI.79.6.3831-3840.2005.
44. Nozawa N, Kawaguchi Y, Tanaka M, Kato A, Kato A, Kimura H, Nishiyama Y. 2005. Herpes simplex virus type 1 UL51 protein is involved in maturation and egress of virus particles. J Virol 79:6947–6956. https://doi.org/10.1128/JVI.79.11.6947-6956.2005.
45. Roller RJ, Haugo AC, Yang K, Baines JD. 2014. The herpes simplex virus 1 UL51 gene product has cell type-specific functions in cell-to-cell spread. J Virol 88:4058–4068. https://doi.org/10.1128/JVI.03707-13.
46. Seo J-Y, Jeon H, Hong S, Britt WJ. 2016. Distinct functional domains within the acidic cluster of tegument protein pp28 required for trafficking and cytoplasmic envelopment of human cytomegalovirus. J Gen Virol 97:2677–2683. https://doi.org/10.1099/jgv.0.000565.
47. Weixel KM, Bradbury NA. 2000. The carboxyl terminus of the cystic fibrosis transmembrane conductance regulator binds to AP-2 clathrin adaptors. J Biol Chem 275:3655–3660. https://doi.org/10.1074/jbc.275.5.3655.
48. Jahnke M, Trowsdale J, Kelly AP. 2012. Ubiquitination of human leukocyte antigen (HLA)-DM by different membrane-associated RING-CH (MARCH) protein family E3 ligases targets different endocytic pathways. J Biol Chem 287:7256–7264. https://doi.org/10.1074/jbc.M111.305961.
49. Bitsikas V, Corrêa IR, Nichols BJ. 2014. Clathrin-independent pathways do not contribute significantly to endocytic flux. eLife 3:e03970. https://doi.org/10.7554/eLife.03970.
50. Le Roy C, Wrana JL. 2005. Clathrin- and non-clathrin-mediated endocytic regulation of cell signalling. Nat Rev Mol Cell Biol 6:112–126. https://doi.org/10.1038/nrm1571.
51. Rodal SK, Skretting G, Garred Ø, Vilhardt F, van Deurs B, Sandvig K. 1999. Extraction of cholesterol with methyl-β-cyclodextrin perturbs formation of clathrin-coated endocytic vesicles. Mol Biol Cell 10:961–974. https://doi.org/10.1091/mbc.10.4.961.
52. Conner SD, Schmid SL. 2003. Regulated portals of entry into the cell. Nature 422:37–44. https://doi.org/10.1038/nature01451.
53. Meissner CS, Suffner S, Schauflinger M, von Einem J, Bogner E. 2012. A leucine zipper motif of a tegument protein triggers final envelopment of human cytomegalovirus. J Virol 86:3370–3382. https://doi.org/10.1128/JVI.06556-11.
54. Hunter T. 2009. Tyrosine phosphorylation: thirty years and counting. Curr Opin Cell Biol 21:140–146. https://doi.org/10.1016/j.ceb.2009.01.028.
55. Galvez T, Teruel MN, Heo W Do, Jones JT, Kim ML, Liou J, Myers JW, Meyer T. 2007. siRNA screen of the human signaling proteome identifies the PtdIns(3,4,5)P3-mTOR signaling pathway as a primary regulator of transferrin uptake. Genome Biol 8:R142. https://doi.org/10.1186/gb-2007-8-7-r142.
56. Byland R, Vance PJ, Hoxie JA, Marsh M. 2007. A conserved dileucine motif mediates clathrin and AP-2-dependent endocytosis of the HIV-1 envelope protein. Mol Biol Cell 18:414–425. https://doi.org/10.1091/mbc.E06-06-0535.
57. Honeychurch KM, Yang G, Jordan R, Hruby DE. 2007. The vaccinia virus F13L YPPL motif is required for efficient release of extracellular enveloped virus. J Virol 81:7310–7315. https://doi.org/10.1128/JVI.00034-07.
58. Archer MA, Brechtel TM, Davis LE, Parmar RC, Hasan MH, Tandon R. 2017. Inhibition of endocytic pathways impacts cytomegalovirus maturation. Sci Rep 7:46069. https://doi.org/10.1038/srep46069.
59. Heineman TC, Connolly P, Hall SL, Assefa D. 2004. Conserved cytoplasmic domain sequences mediate the ER export of VZV, HSV-1, and HCMV gB. Virology 328:131–141. https://doi.org/10.1016/j.virol.2004.07.011.
60. Husain M, Moss B. 2003. Intracellular trafficking of a palmitoylated membrane-associated protein component of enveloped vaccinia virus. J Virol 77:9008–9019. https://doi.org/10.1128/JVI.77.16.9008-9019.2003.
61. Sivan G, Weisberg AS, Americo JL, Moss B. 2016. Retrograde transport from early endosomes to the trans-Golgi network enables membrane wrapping and egress of vaccinia virions. J Virol 90:8891–8905. https://doi.org/10.1128/JVI.01114-16.
62. Grosenbach DW, Ulaeto DO, Hruby DE. 1997. Palmitylation of the vaccinia virus 37-kDa major envelope antigen: identification of a conserved acceptor motif and biological relevance. J Biol Chem 272:1956–1964. https://doi.org/10.1074/jbc.272.3.1956.
63. Sinzger C, Hahn G, Digel M, Katona R, Sampaio KL, Messerle M, Hengel H, Koszinowski U, Brune W, Adler B. 2008. Cloning and sequencing of a highly productive, endotheliotropic virus strain derived from human cytomegalovirus TB40/E. J Gen Virol 89:359–368. https://doi.org/10.1099/vir.0.83286-0.
64. Tischer BK, Von Einem J, Kaufer B, Osterrieder N. 2006. Two-step Red-mediated recombination for versatile high-efficiency markerless DNA manipulation in *Escherichia coli*. Biotechniques 40:191–197.
65. Chevillotte M, Landwehr S, Linta L, Frascaroli G, Luske A, Buser C, Mertens T, von Einem J. 2009. Major tegument protein pp65 of human cytomegalovirus is required for the incorporation of pUL69 and pUL97 into the virus particle and for viral growth in macrophages. J Virol 83:2480–2490. https://doi.org/10.1128/JVI.01818-08.
66. Buser C, Walther P, Mertens T, Michel D. 2007. Cytomegalovirus primary envelopment occurs at large infoldings of the inner nuclear membrane. J Virol 81:3042–3048. https://doi.org/10.1128/JVI.01564-06.
67. Walther P, Ziegler A. 2002. Freeze substitution of high-pressure frozen samples: the visibility of biological membranes is improved when the substitution medium contains water. J Microsc 208:3–10. https://doi.org/10.1046/j.1365-2818.2002.01064.x.
68. Cappadona I, Villinger C, Schutzius G, Mertens T, von Einem J. 2015. Human cytomegalovirus pUL47 modulates tegumentation and capsid accumulation at the viral assembly complex. J Virol 89:7314–7328. https://doi.org/10.1128/JVI.00603-15.
69. Edgar RC. 2004. MUSCLE: multiple sequence alignment with high accuracy and high throughput. Nucleic Acids Res 32:1792–1797. https://doi.org/10.1093/nar/gkh340.